TRANSACTIONS OF THE INSTITUTE OF FLUID-FLOW MACHINERY

No. 132, 2016, 3–15

Bolesław G. Gireń[a,b*], Marzena Noińska-Macińska[b]

Cavitation erosion regimes — an atempt of deriving classification predictor

[a] *Institute of Fluid Flow Machinery, Polish Academy of Sciences, 80-231 Gdańsk, Fiszera 14, Poland*

[b] *University of Economics, 85-229 Bydgoszcz, Garbary 2, Poland*

Abstract

Analysis of the cumulative cavitation erosion curves leads to the inkling that material destruction may be controlled by hardening *ab initio*, hence one can regards the process runs in hardening regime or may be determined by hardening processes only after some time from the beginning of the erosion, i.e., implying the process proceeds in fatigue dominant regime in the initial stages. Verification of material damage susceptibility on the variations of parameters referring to fatigue strength or material ability to mechanical hardening without changing other parameters is almost unfeasible. The method of resolving the cavitation erosion regime for given material has been proposed. The major role of fatigue strength and hydrogen diffusivity at normal temperature in the process was assumed. The scope of the work covers determining the auxiliary parameter values for selected erosion curves obtained under the ICET Programme and referring them to fatigue strength and hydrogen diffusivity of the materials employed, which led to constituting the classification predictor.

Keywords: Cavitation erosion; Erosion regimes; Random processes

1 Introduction

A great concern of numerous researchers and users of liquid-flow systems is to control cavitation phenomena and cavitation erosion process. Preliminary prediction of the erosion performance may be supportive in designing material-loading

*Corresponding Author. Email adress: giren@imp.gda.pl

systems as well as helpful for optimal maintenance of the devices and machines. Evolution of the material deformation and mass loss under discernible cavitation impulses in the field conditions cannot be traced in real time due to randomness of the loadings, both with respect to their power and structure. However, the erosion should be dealt with as a resultant effects of both the impulse actions and the material appropriate reaction. The latter determines the way of solid degradation and susceptibility of the process on given strength or other physical parameters. One of the problems the researchers face to is to distinguish the regimes of the erosion and to reveal the decisive factors for its efficiency. Apart from fatigue and hardening regimes, the evidences on occasionally predominant influence of hydrogen on the rate of material degradation were recognised. In special cases the process may be driven by hydrogen presence, as a result of the forced diffusion from the environmental medium during the implosions of the cavitation bubles [1,2]. Nevertheless, in numerous cases the cavitation erosion process is of fatigue nature – cavitation damage is strongly correlated with fatigue strength of the material [3–9]. Otherwise, if the local brittleness is caused by hardening process, the erosion is conducted under hardening regime, which was confirmed experimentally [10]. Fatigue and hardening regimes should be regarded complementary.

In the paper the classification predictor for cavitation erosion regimes has been proposed and quantified on basis of the International Cavitation Erosion Test (ICET) results [11,12], and completed with the own investigation. Its dependence on the fatigue strength and on the hydrogen diffusivity were determined. Moreover, the dependence of the predictor on the impulse level, loading intensity and fatigue strength of the material was discussed.

2 Aim and scope

The aim of the study was to propose the method of resolving the cavitation erosion regimes for given material, assuming the major role of fatigue strength and hydrogen diffusivity. The scope of the work covers determining the auxiliary parameter values for selected erosion curves obtained under the ICET Programme and referring them to fatigue strength, S_f, and hydrogen diffusivity, D, of the materials employed. This approach leads to constituting the classification predictor, where hydrogen diffusivity has been introduced as a correction. Presented discussion is confined with cases used in the analysis only. The reliability of the method and sources of uncertainties are also discussed.

3 Methodological concept

Damage of the solid under cavitation loading can be quantified by measuring the material volume loss over time in order to obtain a cumulative erosion characteristics. There can be distinguished three stages of degradation process: the stage of plastic deformations and cracking inception (incubation period), the stage of accelerated material disintegration and the stage of the steady-state erosion [13]. In many cases inhibiting processes are absent or appear parallel to the disintegration processes, than retarding of the erosion rate is not reflected in the cumulative curve course. Disintegration and inhibiting process may not develop simultaneously and in numerous cases hardening is delayed with respect to the damage processes, thus quasi-equillibrium state is reached after the accelerated stage of the erosion. The cavitation erosion characteristics for these two cases are shown schematically in Figs. 1a and b.

In order to find the predictor for classification of the process, a new auxiliary parameter W is introduced:

$$W = (x_h - x + y)/x_h \ , \tag{1}$$

where x_h stand for the abscissa of the point on the graph, at which the accelerated erosion stage converts to the steady-state erosion process, and x, y are the coordinates of the point at which the line tangent to the straight part of the erosion curve (steady-state erosion part) cuts the ordinate or abscissa (Figs. 1a and b).

Herein, it is assumed that fatigue to hardening regime change occurs if the tangent line to the straight part of the erosion curve cross the point (0,0). This implies that $W = 1$. The erosion performance presented in Fig. 1a indicates the delayed activation of the hardening effects, than it is a case of fatigue regime of material disintegration ($W > 1$). Otherwise, the curve in Fig. 1b prove the parallel occurrence of the subprocesses, that is the existence of the hardening regime ($W < 1$).

Assuming that parameter W depends on the fatigue strength of the material as well as hydrogen diffusivity ($W = f(S_f, D)$), it can be expressed according to the arbitrarily postulated formula

$$W = f\left(\frac{S_f}{S_{f_{ref}}}\left(1 - \frac{\gamma}{\log D}\right)\right) \ ; \tag{2}$$

here the function symbol f represents experimentally determined relationship between the W parameter and the values of expression $(S_f/S_{f_{ref}})(1-\gamma/\log D)$, S_f and $S_{f_{ref}}$ are the fatigue strength and reference fatigue strength, respectively, D is

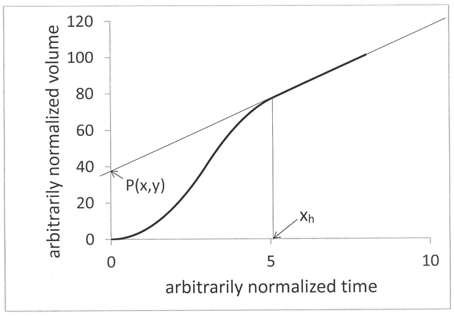

a)

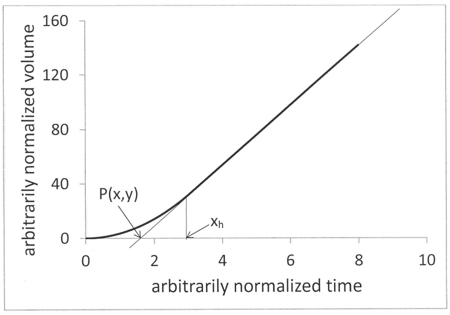

b)

Figure 1: Two types of cavitation erosion curves under considering. The variables designation are presented.

the hydrogen diffusivity, and γ is the phenomenological impact coefficient which may be derived experimentally by comparison of the results obtained in different environmental conditions, at different hydrogen supply. The rough reasoning was as follows:

	Increase in S_f results in	Increase in D causes
Energy threshold for damage	increase	decrease
Dissipation of the energy absorbed	increase	decrease
Hardening ability	(*)	decrease

(*) nonlinear indirect relationship to other parameters

Eventual calibration of the coefficient γ should be carried out according to phenomenological procedures: in environmentals deprived of hydrogen or rich of hydrogen content.

4 Data sources

In calculations the cumulative erosion curves of five tested materials have been used: aluminium alloy PA2 (Mg 2.7, Al rest); brass M63 (Zn 32.6, Cu rest); Armco iron E04 (C 0.035, Mn 0.1, Si 0.01, P 0.026, S 0.035, Fe rest); carbon steel 45 (C 0.43, Mn 0.63, Si 0.26, P 0.03, S 0.033, Fe rest); 1H18N9T acid resistant steel (C 0.4, Mn 1.37, Si 0.55, P 0.03, S 0.01, Cr 17.6, Ni 9.4, Ti 0.6, Fe rest). Their designations follow Polish Standards. Detailed information on heat treatment conditions and mechanical properties as well as description of the test facilities are to be found in [11,12]. Summary data are given in Tab. 1.

Table 1: Test conditions for different test facilities [12].

Test conditions for vibratory rigs					
Laboratory	Frequency, kHz	Peak-peak, μm	Specimen size, mm	Temperature, °C	Horn tip/sample gap, mm
CISE	20	50.8	15.8	22	–
CSSRC	20	32	16	20	–
HIRO	19.9	24	16	40	–
IMP	8.1	50	12.5	20	–
TSING	19.8	35	19.5	15–20	–
VSB	20	40	16	20	–
IWP	22	25	16	20	–
CAP stationary	20	60	10	30	0.35
HIRO stationary	19.9	28	16	40	0.4
HULL stationary	20	117	16.7	20	0.5
VSB stationary	20	40	16	20	1
Test conditions for cavitation tunnels					
Laboratory	Cavitator	Liquid velocity upstream, m/s	Liquid velocity critical, m/s	Upstream pressure, kPa	Temperature, °C
CITY	Wedge	21	45	890	40
CSSRC	Bolt	14	28	103	20
HAN	Barricade	40	670	700	22
HIRO	Barricade	30	300	405	40
IWP	–	–	–	1260	16
PEITZ	Bolt	30	41	930	10
Test conditions for rotating disks facilities					
Laboratory	Cavitator	Cavitator velocity, m/s	Disk dia., mm	Mean pressure, kPa	Temperature, °C
CSSRC	Hole	43	350	103 (absolute)	20
IMP	Bolt	42.5	330	155 (gauge)	20
KSB	Bolt	29.6	500	46 (absolute)	40
SIGMA	Hole	60.2	275	70 (gauge)	40
Test conditions for cavitating jet (CJ) and (LJ) facilities					
Laboratory	Nozzle dia., μm	Jet velocity, m/s	Pressure upstream, MPa	Pressure downstream, MPa	Temperature, °C
FCRI – CJ	397–424	90–98	21	0.14	28
HAN – CJ	400	–	14–19	0.1	24
SIGMA – LJ	6000	6.75	0.126	0.1	

Strength parameters of the materials are pooled in Tab. 2. Apart from the ICET data, the results of the own experimental investigations on electrolytic copper erosion exposed to intense cavitation loadings at the rotating disc facility were also used (Fig. 2). From provided by the ICET only curves of sufficient long time of exposition were included to analysis for it guarantee the proper interpretation of each revealed stage of the erosion. Data on the hydrogen diffusivity in materials tested are gathered in Tab. 3.

Table 2: Strength parameters of the materials.

Material	PA2	M63	E04	Steel 45	1H18N9T	M1E	Designation
Density, g/cm^3	2.69	8.43	7.85	7.87	7.88	8.43	ρ
Vickers hardness HV$_{10}$	71.7	80.9	108.4	192.8	191	50	HV
Tensile strength, MPa	208	352	328	721	605	248	T_S
Yield point, MPa	169	117	263	419	225	75	s^e
Fatigue strength, MPa	110	140	199	278.5	485	64	S_f
Ultimate strain, %	17	65	40,5	22	52	34	s
Hardening exponent, –	0.17	0.35	0.23	0.21	0.54	0.48	n
Modulus of elasticity, GPa	70	99	210	210	200	110	E

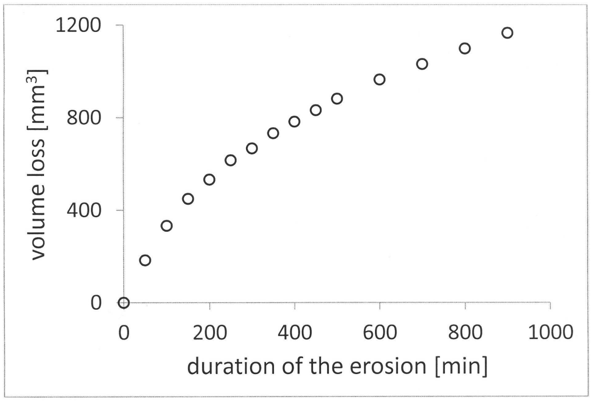

Figure 2: Volume loss of copper ME1 samples as a function of exposition time at the rotating disc rig in the IMP PAN.

Table 3: The hydrogen diffusivity in materials.

Material	Hydrogen diffusivity, cm^2/s	Temperature, °C	Ref.
Aluminium PA2	4.2×10^{-7} (average)	50	[14,15]
Alpha-brass (*)	7.82×10^{-3}	500–730	[16]
Armco iron	5×10^{-5}	27	[17,18]
Steel 45	9×10^{-6}	room	[19]
Steel 304	3.5×10^{-12} (average)	25	[20,21]
Copper	2×10^{-10} (average)	50	[22–25]

(*) In calculations conducted in present paper the value of diffusivity equal 7.82×10^{-4} has been used after extrapolation to the temperature 50 °C.

5 Breakdown of the results

The comparison of average W values of strong – high amplitude impulses (labs: SIGMA LJ, HAN CJ, SIGMA RD, IMP VR) and weak – low amplitude impulses (labs: CSSRC VR, HIRO VRS) has been made. Loading intensities of the particular fractions of the pressure impulses are given in Tab. 4. The presented selection was accomplished basing on the results of calculations of each loading fraction carried out by dr J. Steller for each ICET participant set-up [26]. The results are shown in Fig. 3. The same comparison has been made with respect to the set-up of high and low intensity loadings and these results are shown in Fig. 4.

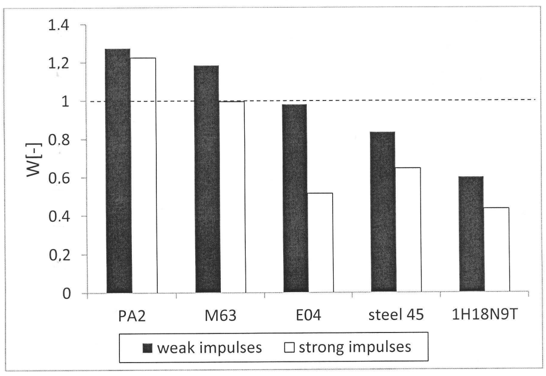

Figure 3: Average values of W parameter determined for set-ups of weak (low) and strong (high) impulse pressure for materials tested in ICET.

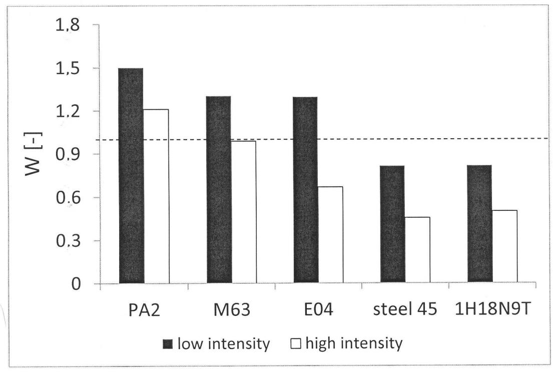

Figure 4: Average values of W parameter determined for set-ups of weak (low) and strong (high) loading intensities for materials tested in ICET.

The dependence of average values of W parameter on fatigue strength of the materials S_f and on parameter $(S_f/S_{f_{ref}})(1-\gamma/\log D)$, of all participating laboratories, are presented in Figs. 5 and 6, respectively. In calculations for the impact coefficient a value $\gamma = 5$ has been adopted.

Substantially higher values of W parameter, determined for set-ups of low impulse pressure (Fig. 3), prove that cavitation erosion under low impulses conditions probably proceeded in different regime than under high impulses conditions. However, the loading intensities were not the same, whereas there is also relationship between W and loading intensity (see Fig. 4).

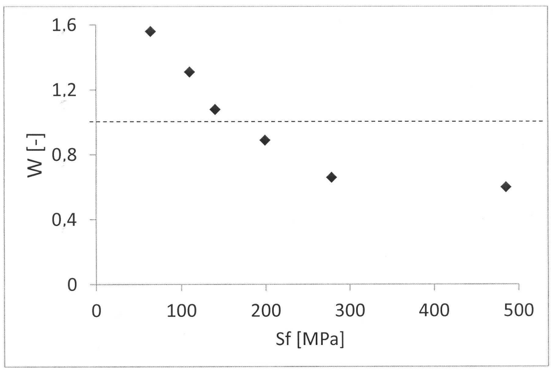

Figure 5: Dependence of W parameter on the fatigue strength, S_f of the material – values of W are the average derived from the ICET results for each particular material.

Table 4: Distributions of the loading intensities with respect to the impulse pressure fractions in MPa, as measured by piezoelectric sensors 105C33 PCB [26].

Laboratory	Material	Loading intensity for particular fractions, W/cm^2						
		0-1 MPa	1-2 MPa	2-4 MPa	4-8 MPa	8-16 MPa	16-32 MPa	> 32 MPa
CSSRC VR	PA	34.8	24.2	15.3	8.8	4.4	2.9	90.4
CSSRC Vr	M6	34.8	24.2	15.3	8.8	4.4	2.9	90.4
CSSRC VR	E0	34.8	24.2	15.3	8.8	4.4	2.9	90.4
CSSRC VR	45'	34.8	24.2	15.3	8.8	4.4	2.9	90.4
CSSRC VR	1H	34.8	24.2	15.3	8.8	4.4	2.9	90.4
HIRO VRS	PA	18.8	12.5	7.5	4.1	1.9	1.1	45.9
HIRO VRS	M6	18.8	12.5	7.5	4.1	1.9	1.1	45.9
HIRO VRS	E0	18.8	12.5	7.5	4.1	1.9	1.1	45.9
HIRO VRS	45'	18.8	12.5	7.5	4.1	1.9	1.1	45.9
HIRO VRS	1H	18.8	12.5	7.5	4.1	1.9	1.1	45.9
IMP VR	PA	0	0	0.6	7.5	40.4	6.4	54.9
IMP VR	M6	0	0	0.6	7.5	40.4	6.4	54.9
IMP VR	E0	0	0	0.6	7.5	40.4	6.4	54.9
IMP VR	45'	0	0	0.6	7.5	40.4	6.4	54.9
IMP VR	1H	0	0	0.6	7.5	40.4	6.4	54.9
IMP RD	PA	0	1.1	11.7	67.2	21.1	0	101.1
IMP RD	M6	0	1.1	11.7	67.2	21.1	0	101.1
IMP RD	E0	0	1.1	11.7	67.2	21.1	0	101.1
IMP RD	45'	0	1.1	11.7	67.2	21.1	0	101.1
IMP RD	1H	0	1.1	11.7	67.2	21.1	0	101.1
SIGMA RD	PA	0	0	0	0.5	1.4	0	1.9
SIGMA RD	M6	0	0	0	0.5	1.4	0	1.9
SIGMA RD	E0	0	0	0	0.5	1.4	0	1.9
SIGMA RD	45'	0	0	0	0.5	1.4	0	1.9
SIGMA RD	1H	0	0	0	0.5	1.4	0	1.9
HAN CJ	PA	0	0	0	0	1.8	1.5	3.3
HAN CJ	M6	0	0	0	0	1.8	1.5	3.3
HAN CJ	E0	0	0	0	0	1.8	1.5	3.3
HAN CJ	45'	0	0	0	0	1.8	1.5	3.3
HAN CJ	1H	0	0	0	0	1.8	1.5	3.3
HAN CJ2	PA	0	0	0.8	2.5	3.2	2.5	9
HAN CJ2	M6	0	0	0.8	2.5	3.2	2.5	9
HAN CJ2	E0	0	0	0.8	2.5	3.2	2.5	9
HAN CJ2	45'	0	0	0.8	2.5	3.2	2.5	9
HAN CJ2	1H	0	0	0.8	2.5	3.2	2.5	9
HAN CJ3	PA	0	0	24	14.3	3.4	4.1	45.8
HAN CJ3	M6	0	0	24	14.3	3.4	4.1	45.8
HAN CJ3	E0	0	0	24	14.3	3.4	4.1	45.8
HAN CJ3	45'	0	0	24	14.3	3.4	4.1	45.8
HAN CJ3	1H	0	0	24	14.3	3.4	4.1	45.8
SIGMA LJ	PA	0	0	0	0.7	81.3	3.1	85.1
SIGMA LJ	M6	0	0	0	0.7	81.3	3.1	85.1
SIGMA LJ	E0	0	0	0	0.7	81.3	3.1	85.1
SIGMA LJ	45'	0	0	0	0.7	81.3	3.1	85.1
SIGMA LJ	1H	0	0	0	0.7	81.3	3.1	85.1

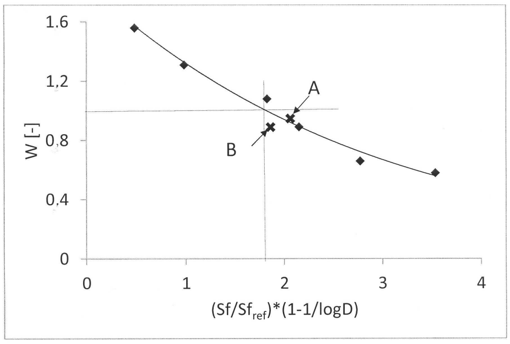

Figure 6: Dependence of W parameter on the parameter $(S_f/S_{f_{ref}})(1 - 5/\log D)$ – values of W are the average derived from the ICET results for each particular material.

As it can be inferred from Fig. 6, the transit value of parameter $(S_f/S_{f_{ref}})(1 - 5/\log D)$, corresponding to value of $W = 1$ is about 1.79. Verification has been made in the cases of chromium steel (2H13) and aluminium bronze (BA1032) subjected to cavitation loadings at the rotating disk rig in the Institute of Fluid-Flow Machinery in Gdańsk. Corresponding values of W parameter (derived from cumulative erosion curves – Figs. 7a and 7b) and parameter $(S_f/S_{f_{ref}})(1-5/\log D)$ are as follow:

Material	S_f, MPa	W	Coordinates of characteristic points on the graph (Fig. 6)
2H13	271	0.97	point A (2.03, 0.97)
BA1032	255	0.85	point B (1.78, 0.85)

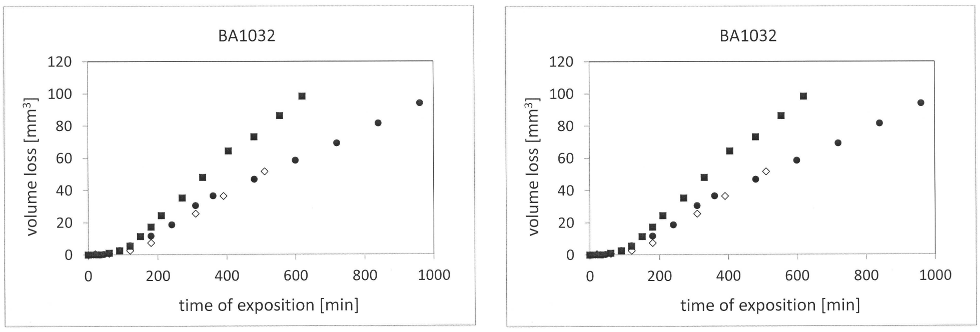

a) b)

Figure 7: Cumulative erosion curves of bronze BA1032 (a) and steel 2H13 (b) subjected to cavitation loadings at the rotating disk rig in the Institute of Fluid-Flow Machinery.

6 Discussion and summary remark

Analysis of the specific nature of material volume loss in time under cavitation loadings leads to the inkling that in case of $W > 1$ the rate of material destruction is determined by hardening processes only after some time from the beginning of the erosion. Therefore, in the initial stages the process proceeds in fatigue dominant regime. If $W < 1$, the erosion is controlled by hardening *ab initio*, hence one can regard the process runs in hardening regime. However, verification of the susceptibility of material damage process on the variations of parameters referring to fatigue strength or material ability to mechanical hardening without changing other parameters is almost unfeasible.

Direct relationship between parameter W and fatigue strength (Fig. 5) comprise the cases of differentiated materials, thus the hypothetical influence of other properties are not revealed. The nature of the dependence of W parameter on fatigue strength, S_f, is not changed substantially if hydrogen diffusivity is taken into account as a corrective factor (Fig. 6), but functional approximation of the W values derived from ICET results becomes more accurate. The values of W derived from the own investigations (materials BA1032 and 2H13) do not confirm precisely the dependence, but are not far beyond its possible uncertainty.

Differentiation of the W values for the cases of weak and strong impulses (Fig. 3) is a result of enhanced ductile deformations under strong impulse action. On the other hand, strong impulse action is accompanied with intensified diffusion of hydrogen which should impair the hardening process and promote fatigue mechanism of the erosion, which is hardly to be detected in Fig. 3. The values of hydrogen diffusivity, D, employed in this investigation may not be adequate to cavitation conditions: the parameter is strongly depend on thermodynamic conditions, therefore there can be essential change in its value under cavitation impulse action. Moreover, the data used are available literature data referring to relative materials, but not exactly the same.

The results shown in Fig. 4 allow to draw conclusion that the higher loading intensity, the more probable run of the process in hardening regime. Moreover, decreasing of the W with an increase in loading intensity indicate the latter may be a scaling factor for the process.

Possible incorrectness of the proper determining the values of W may result from significant diversity of the cumulative erosion characteristics obtained in the ICET Programme as well as not sufficient time of exposition in some cases. Some of the curves used for analysis do not ensure the steady state stage of the erosion was achieved.

Considerations on the cavitation erosion regimes based only on the analysis of the cumulative erosion curves leads to the conclusion that there is rather no precise critical value of the classification predictor referring to fatigue to hardening regime change, therefore obtained value 1.79 is only approximate assessment.

Received 29 November 2015, revised form 2 June 2016

References

[1] Balyts'kyi O.I., Chmiel J., Krause P., Niekrasz J.: *Role of hydrogen in the cavitation fracture of 45 steel in lubricating media*. Mater. Sci. **45**(2009), 5, 651–654.

[2] Balyts'kyi O.I., Chmiel J., Dorobczyński L.: *Analysis of electrochemical oscillations under conditions of vibration cavitation*. Mater. Sci. **47**(2011), 1, 21–25.

[3] Heymann F.J.: *On the time dependence of the rate of erosion due to impingement or cavitation, erosion by cavitation or impingement*. ASTM Spec. Techn. Pub. **408**(1967), 70–110.

[4] Richman R.H., McNaughton W.P.: *Correlation of cavitation erosion behaviour with mechanical properties of metals*. Wear **140**(1990), 1, 63–82.

[5] Richman R.H., McNaughton W.P.: *A metallurgical approach to improved cavitation-erosion resistance*. J. Mater. Eng. Perform. **6**(1997), 5, 633–641.

[6] Bedkowski W., Gasiak G., Lachowicz C., Lichtarowicz A., Lagoda T., Macha E.: *Relations between cavitation erosion resistance of materials and their fatigue strength under random loading*. Wear **230**(1999), 2, 201–209.

[7] Ahmed S.M., Hokkirigawa K., Ito Y., Oba R.: *Scanning electron microscopy observation on the incubation period of vibratory cavitation erosion*. Wear **142**(1991), 2, 303–314.

[8] Hattori S., Nakao E.: *Cavitation erosion mechanisms and quantitative evaluation based on erosion particles*. Wear **249**(2002), 10-11, 839–845.

[9] Fortes-Patella R.,Reboud J.L.: *A new approach to evaluate the cavitation erosion power*. J. Fluid Eng.-T ASME **120**(1998), 2, 335–344.

[10] Giren B.G.: *Material proprieties essential for cavitation erosion of laser produced surface alloys*. J. Mater. Sci. **39**(2004), 1, 295–297.

[11] Steller J.: *International cavitation erosion test and quantitative assessment of material resistance to cavitation*. Wear **233-235**(1999), 51–64.

[12] Steller J., Gireń B.G.: *International Cavitation Erosion Test. Final Report.* Bull. IFFM PAS. 560/1519/2015, Gdańsk 2015.

[13] Reymann Z., Steller K.: *Assessment of material resistance on the action of flow induced cavitation*. Transactions IFFM **76**(1978), 95–125 (in Polish).

[14] Hayashi Shin-Ichirou: *Measurement of hydrogen diffusivity in aluminum and a dilute alloy by thermal evolution spectroscopy*. Jpn. Appl. Phys. **37**(1998), 1, 3A, (http://iopscience.iop.org/article/10.1143/JJAP.37.930/pdf).

[15] Young G.A. Jr., Scully J.R.: *The diffusion and trapping of hydrogen in high purity aluminium*. Acta Materialia **46**(1998), 18, 6337–6349.

[16] Caskey G.R. Jr, Derrick R.G.: *Hydrogen permeability through alpha-brass.* Metall. Trans. A, **8**(1977), 3, 511–513.

[17] Lukezich S.J., Wilde B.E.: *Corrosion behaviour of nickel-base high performance alloys in simulated repository environments.* MS thesis, The Ohio State University, 1989.

[18] Chene J., Brass A.M.: *Interactions Hydrogčne-Métal en relations avec le processus de corrosion souscontrainte.* In: Corrosion sous contrainte, phénoménologie et mécanisme (D. Desjardins, R. Oltra, Eds.). Editions de Physique, 1992, 159–210.

[19] Sakamoto Y., Mantani T.: *Effect of quenching and tempering on diffusion of hydrogen in carbon steel.* T. Jpn. I. Met. **17**(1976), 11, 743–748.

[20] Palmer Andrew C., King Roger A.: *Subsea Pipeline Engineering.* PennWell Corp., Tulsa 2008.

[21] Murakami Y., Kanezaki T., Mine Y., Matsuoka S.: *Hydrogen embrittlement nechanism in fatigue of austenitic stainless steels.* Metall. Mat. Trans. A, **39**(2008), 6, 1327–1339.

[22] Gdowski C.E., Bullen D.B.: *Survey of Degradation Modes of Candidate Materials for High-Level Radioactive-Waste Disposal Containers, Vol.6 Effects of Hydrogen in Austenitic and Copper-Based Alloys*, LLNL, Livermore 1988.

[23] Magnusson H., Frisk K.: *Self-diffusion and impurity diffusion of hydrogen, oxygen, sulphur and phosphorus in copper.* Techn. Rep. TR-13-24, Svensk Kärnbränslehantering AB, 2013.

[24] Ishikawa T., McLelJan R.B.: *The diffusivity of hydrogen in copper at low temperatures.* J. Phys. Chem. Solids **46**(1985), 4, 445–454.

[25] Sakamoto Y., Takao K.: *The electrochemical determination of diffusivity and solubility of hydrogen in copper.* T. J. Jpn. I. Met. **46**(1982), 3, 285–290.

[26] Steller J.: *Cavitation loading at test rigs used in International Cavitation Erosion Test.* IMP PAN Rep. 213/2014, Gdańsk 2014 (in Polish).